Compact and Planar End-Fire Antenna for PicoSat and CubeSat Platforms to Support Deployable Systems

VICTORIA GÓMEZ-GUILLAMÓN BUENDÍA[1] **(Member, IEEE),**
SYMON K. PODILCHAK[2] **(Senior Member, IEEE), SALVATORE LIBERTO**[3] **(Student Member, IEEE),**
TOM WALKINSHAW[4]**, CONSTANTIN CONSTANTINIDES**[4]**,**
DIMITRIS E. ANAGNOSTOU[3] **(Senior Member, IEEE), GEORGE GOUSSETIS**[3] **(Senior Member, IEEE),**
AND MAARTEN VAN DER VORST[5]

[1]Radar Technology Department, TNO, 2597 AK The Hague, The Netherlands

[2]School of Engineering, The Edinburgh University, EH8 9YL Edinburgh, U.K.

[3]Institute of Sensors, Signals, and Systems, School of Engineering and Physical Sciences Edinburgh Campus, Heriot–Watt University, EH14 4AS Edinburgh, U.K.

[4]Alba Orbital, G5 9EP Glasgow, U.K.

[5]Antenna Section, ESA-ESTEC, 2201 AZ Noordwijk, The Netherlands

CORRESPONDING AUTHOR: S. K. PODILCHAK (e-mail: s.podilchak@ed.ac.uk)

ABSTRACT A miniaturized planar Yagi-Uda antenna for integration with PicoSats or other SmallSat missions is proposed. Miniaturization techniques, such as meandering and 1-D artificial dielectric concepts to reduce the guided wavelength, are employed to overcome space constraints imposed by the SmallSat footprint while still maintaining good performance for the FR-4 antenna. Simulations and measurements have been carried out on the Unicorn-2 PicoSat chassis from Alba Orbital and are in good agreement. Also, antenna dimensions have been reduced between 15% and 66% when compared to a more conventional planar Yagi-Uda antenna working at the same frequency. This compactness allows for simple integration with the deployable solar panel array of the Unicorn-2 PicoSat spacecraft. Full end-fire radiation is achieved and peak gain values are about 5 dBi for the antenna when fully integrated on the satellite chassis, offering an attractive solution for downlink connectivity. This compact antenna design can also be used within an array for beam steering or integrated within the solar cell modules of other PicoSats, CubeSats and SmallSats. Applications include Earth observation, remote sensing, as well as SmallSat to ground station communications. The planar Yagi-Uda antenna may also be useful wherever end-fire radiation is required from a compact antenna structure.

INDEX TERMS Planar Yagi-Uda, artificial dielectrics, CubeSat, deployable systems, solar panel arrays.

I. INTRODUCTION

COMMERCIAL missions employing SmallSats, such as CubeSats and PicoSats, are becoming more common. This is due to the demands for low-cost and compact space platforms which can offer Earth observation (EO) and diverse communication services whilst also providing connectivity with other satellites [1], [2]. This augmented demand, as compared to more conventional satellites, translates in more payload systems integrated into the SmallSat, causing a high density of mechanical and electrical subsystems. This is a challenge for space engineers as the available surface and volume is more and more limited, while there are also weight and cost constraints to consider.
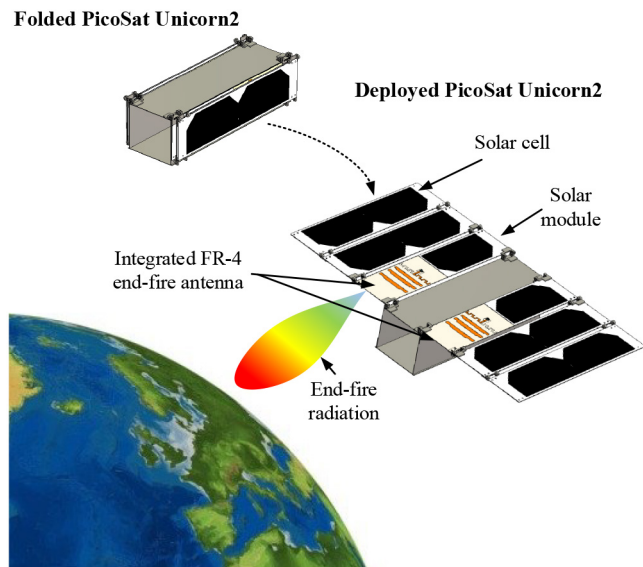
Folded PicoSat Unicorn2

One key element of any payload offering different communication services is the antenna. Suitable beam pattern characteristics are also vital to maintain communications. In EO for instance, the power radiated from the antenna is required to be directed towards the Earth for data exchange, as depicted in Fig. 1. Depending on the required location of the antenna and how the satellite has been designed or is to be positioned in space, antenna selection may be limited when iso-flux, broadside or end-fire radiation patterns are required. Keeping these antennas compact, low-cost and lightweight is critical specially in missions where the wavelength can be large in comparison with the available footprint. As a result, designs based on turnstile monopoles, helix antennas [3], [4], or metallic and PCB-based structures [5], [6] may be considered.

Depending on the gain requirements, deployable antennas are versatile structures with a wide variety of applications not only limited to low frequencies. Antenna systems, as in [8], [9], based on reflectors for high frequency bands, were achieved with meshed or inflatable antennas. Although these deployable systems can make optimum use of the footprint in SmallSats for large antennas, the required stowage volume, and at times, the complicated deployment mechanisms can limit commercial and industrial adoption. On the other hand, low-cost planar solutions, despite typically providing moderate gain values, can be a reliable and more low-profile alternative. Furthermore, they have more degrees of freedom in terms of design flexibility. In this respect, integrating the antenna on the solar modules [10], [11], [12], [13], [14] is an attractive option to optimize the available space on the SmallSat whilst not requiring any specific deployment mechanism for the antenna itself.

In the Solant project [10], crossed slots were etched on amorphous silicon solar cells to achieve circularly polarized (CP) broadside radiation. This antenna design set the precedent for future configurations taking advantage of the available surface on the solar modules [11]. Conventional and modern techniques, such as grid antennas [12], [13], [14] or transparent conductors [15], [16], are enabling new planar structures which use the solar cell layer as the antenna substrate. This can avoid the perforation or relocation of the solar modules [17] whilst maintaining solar power harvesting capabilities. However, these antennas may provide lower efficiencies, which can be critical in the case of transparent conductors, since the conductivity can be of order 10^6 or 10^5 S/m depending on the employed conductive oxide [16]. Moreover, when full end-fire radiation is needed, antenna integration on top or near the solar cells might not be easily feasible. This is mainly due to the continuous ground plane needed under the thin solar cells (required for proper DC biasing and solar power collection circuitry) which could short-circuit important antenna elements. In this case, antenna radiation can be limited to quasi-end-fire or near broadside [18]. One solution is the removal of one of the solar cells to use the substrate underneath and pattern it as desired using conventional PCB design approaches. In this way, full end-fire radiation can more easily be achieved by using a variety of printed elements.

When requiring CP radiation at end-fire, antipodal configurations as in [19], [20], [21] could be considered. In these structures, complementary magnetic dipoles and mirrored open loops etched on top and bottom of the substrate are required. However, these designs provide optimum performance involving low permittivity substrates ($\varepsilon_r = 1.1$). If considered for PicoSat or CubeSat integration, higher permittivities might be needed depending on the antenna design frequency. This size constraint can result in a lower radiation efficiency or reduced CP performance due to volume restrictions. In particular, antenna thickness requirements need to be on the order of $0.05\lambda_0$ [19], [20], [21]. Moreover, such a physical requirement might make SmallSat integration, when operating in the L- or S-bands, not easily feasible, and, without the adoption of some vertical substrate thickness reduction technique or advanced antenna miniaturization.

Linear polarized (LP) antennas instead could be investigated when the possible antenna size and thickness is limited as is the case for the deployable solar cell array on the Unicorn-2 Picosat from Alba Orbital (see Fig. 1). When considering planar design solutions, there are a number of miniaturization techniques. Meandering of microstrip, the use of artificial magnetic materials [22], [23] or artificial dielectrics [24], can be considered for such SmallSat antenna integration. For end-fire radiation, conventional Yagi-Uda antennas or arrays, based on microstrip dipoles [25], can also be implemented and miniaturized to satisfy the size and operating frequency requirements [18]. For example, the preliminary investigations in [18] showed promising simulations where a full metallic chassis was assumed. In this case, the beam was diverted away from end-fire but gain values were kept around 3 dBi.

Some other works have also investigated planar Yagi-Uda antennas for SmallSats. For instance, [26] reported a 6 dBi printed Yagi-Uda array for 2.45 GHz and was simulated on the chassis of a 3U CubeSat. This antenna design with no miniaturization, needed a substrate of $90 \times 150 \, \text{mm}^2$ which could be too large for any PicoSat with additional payloads. This led to a modified version in [27] where copper rods embedded in a FR-4 substrate, formed a Yagi-Uda array that was mechanically steered to control the beam in the elevation plane. This might increase the complexity and cost, whilst needing the satellite to have the solar panels facing the Earth to achieve full end-fire radiation. However, this would prevent efficient power harvesting from the Sun.

Some techniques have also been reported for planar Yagi-Uda miniaturization include meandering, C-shaped elements, and folded dipoles [28], [29], [30], [31]. Despite providing some design compactness, the size reduction was not significant, and in most cases, the number of directors were sacrificed due to space constraints resulting in low gain performances. On the other hand, a compact structure which maintained directivity was achieved using an intricate technique; i.e., parasitic interdigitated strips as in [32], which required some complex and design-specific loading considerations.

Advancing on these developments whilst providing an alternative design approach, we propose a miniaturized planar Yagi-Uda antenna structure based on low-cost PCB technology. The design achieves full end-fire radiation in the S-band and is fully integrated within the solar panel array, and this array extends from the PicoSat Chassis (see Fig. 1). In particular, structure meandering and artificial dielectric concepts were employed by loading the three directors of the planar antenna (see Fig. 3) in a 1-D sequence to achieve overall structure compactness whilst maintaining directivity. This advances on our preliminary simulation work in [18], which mainly reported the design of a Yagi-Uda-like structure using an array of microstrip patches for operation at 8 GHz for placement on the glass layer of a solar cell.

To the best of the Authors' knowledge, 1-D artificial dielectric concepts and meandering have not been effectively applied on fully planar Yagi-Uda antennas previously. These miniaturization techniques are newly adopted in this paper, mainly, in an effort to fit the proposed S-band end-fire antenna on the deployable solar panel array of the Unicorn-2 Picosat (see Figs. 1 to 3). These techniques are further described in Section II together with a comparison with a conventional Yagi-Uda design, where some important dimensions have been reduced by more than 65% whilst still maintaining an operating bandwidth of more than 6%. It will also be shown that our compact design achieves a 40% and 15% reduction of the total required antenna length and width, respectively, when compared to a more conventional and non-compact version. Simulated results will also be discussed in Section II, including the scenario were the antenna is in frees-space and integrated onto the Unicorn-2 PicoSat. Measured results are reported in Section III with a summary in Section IV.
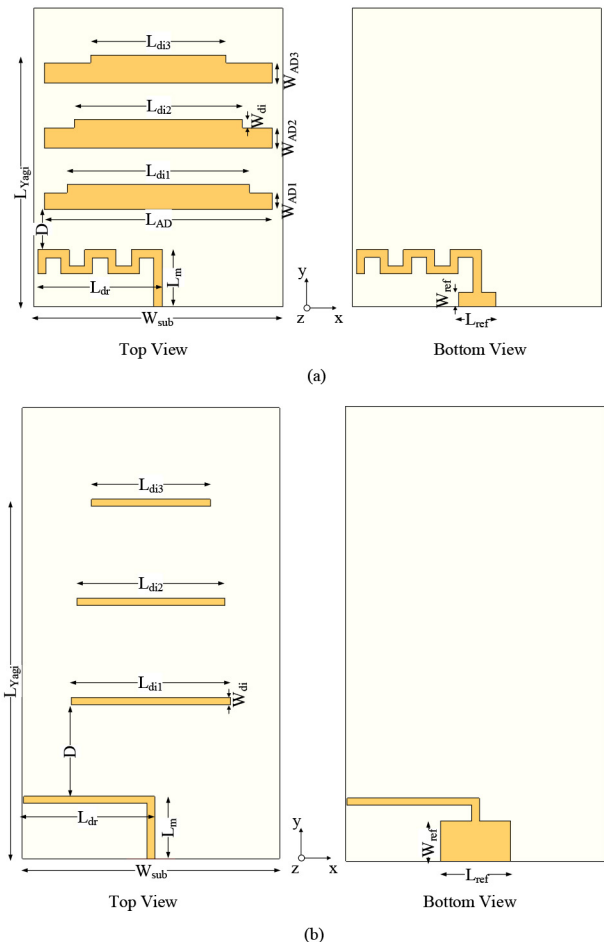
FIGURE 2. Top and bottom views for: (a) the proposed 2.4 GHz planar Yagi-Uda antenna with artificial dielectric loading and meandering implemented using a 0.4 mm thick FR-4 substrate; (b) a conventional printed Yagi-Uda antenna for 2.4 GHz for comparison.

II. ANTENNA DESIGN AND SIMULATIONS

Typical antenna performance specifications for EO down-link transmission in the S-band for the Unicorn-2 PicoSat commercial mission [7] are an optimum LP gain of 5 dBi and a minimum -10 dB impedance reflection coefficient bandwidth of 10 MHz (0.42%) [18].

For the Unicorn-2 PicoSat, the chassis has already most of its space occupied with other payloads [7]. Thus, the integration of a new antenna was limited to the solar module nearest the main body of the satellite of the deployable wings (see Figs. 1 and 4, inset). These solar modules were constructed using epoxy resin material, defining the antenna substrate. Also, due to the need to maintain a weight balanced PicoSat structure, removal of one of the solar cells on the other side of the chassis was required and a second end-fire antenna can be added (see Fig. 1). Also, when the solar cell is removed and the epoxy substrate is used for antenna integration, the available footprint [7] is $43.80 \times 90 \, \text{mm}^2$ with a substrate thickness of 0.4 mm. This defines the available footprint for our miniaturized end-fire antenna which must operate at 2.4 GHz for ground station connectivity. Using

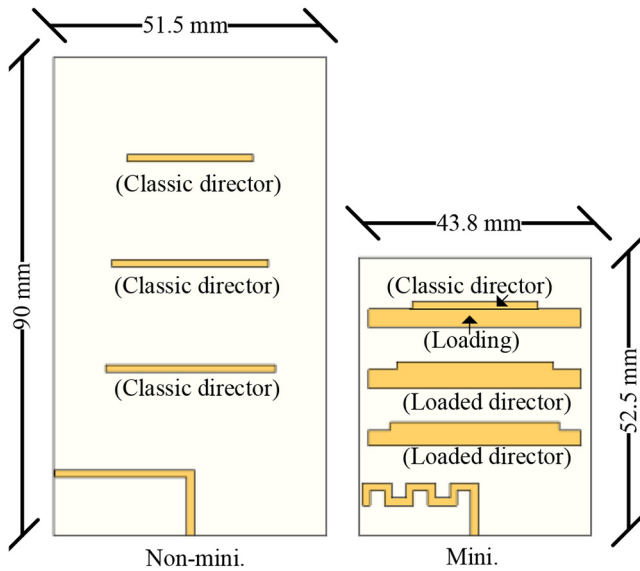**TABLE 1.** Yagi-Uda original & miniaturized parameters.

	L_{yagi}	L_{dr}	L_m	D	L_{AD}
Conventional	$0.58\lambda_0$	$0.21\lambda_0$	$0.1\lambda_0$	$0.15\lambda_0$	-
Miniaturized	$0.35\lambda_0$	$0.17\lambda_0$	$0.08\lambda_0$	$0.06\lambda_0$	$0.32\lambda_0$

	L_{di1}	L_{di2}	L_{di3}	L_{ref}	W_{sub}
Conventional	$0.26\lambda_0$	$0.24\lambda_0$	$0.19\lambda_0$	$0.11\lambda_0$	$0.41\lambda_0$
Miniaturized	$0.26\lambda_0$	$0.24\lambda_0$	$0.19\lambda_0$	$0.05\lambda_0$	$0.35\lambda_0$

	W_{di}	W_{AD1}	W_{AD2}	W_{AD3}	W_{ref}
Conventional	$0.01\lambda_0$	-	-	-	$0.06\lambda_0$
Miniaturized	$0.01\lambda_0$	$0.02\lambda_0$	$0.03\lambda_0$	$0.03\lambda_0$	$0.02\lambda_0$

FIGURE 3. The non-miniaturized (conventional) and miniaturized designs for size comparison illustrating a reduction of more than 40%.

FR-4 material enables low-cost experimental demonstration and proof-of-concept for the space-ready antenna.

A. DESIGN CONSIDERATIONS

This antenna is composed of several parasitic microstrip dipoles [25] acting as directors, which are typically placed at a distance of $0.15 - 0.3\lambda_0$ from the driven element and other directors [33]. Classic and well known formulas for Yagi-Uda antennas [33] were initially used to obtain the parameters of the non-miniaturized version (see Fig. 2 (b)) which is the starting point in our design process. Relevant dimensions are outlined in Figs. 2 (a) and (b) and Table 1. The antenna is fed by a 50-Ω microstrip line and has been modelled and simulated in CST [34].

In order to achieve a higher gain, more directors are exploited. However, the length of the available footprint is very limited (90 mm or $0.72\lambda_0$ where λ_0 is the free-space wavelength at the design frequency of 2.4 GHz) and cannot accommodate many directors to comply with the required

5 dBi realized gain requirement. Given this space available, the substrate losses whilst considering conventional design approaches, the maximum gain achievable is 3 dBi. Also, size constraints do not permit a fourth director to increase gain. Nevertheless, this would still not comply with gain requirements for the Unicorn-2 PicoSat mission. In addition, to improve the matching, the feeding microstrip line L_m of the non-miniaturized version should be larger than $0.1\lambda_0$ (optimally around $0.25\lambda_0$, as in [18]). Moreover, the length of the driven element L_{dr} needed to operate at 2.4 GHz, and it could not fit within the substrate width (W_{sub} = 43.80 mm). For these two reasons and to comply with the antenna requirements, several miniaturization techniques were adopted.

Adapting the driven element into the constrained width W_{sub} was achieved using meandering and its length L_{dr} was physically miniaturized to maintain operation at 2.4 GHz. This meandering reduced the width of the proposed Yagi-Uda by about 15%. On the other hand, the distance between directors D can also be reduced by applying artificial dielectric concepts [24], realized by local printed inclusions. This achieves a representative 1-D configuration for guided wavelength reduction along the y-direction and near the driven and director elements. Accordingly, the surface reactance near the printed metallic segments is locally tailored to achieve a higher effective relative permittivity, as in [24], [35], [36], allowing for the reduction of the distance D. For example, the minimum ($D = 0.15\lambda_0$) required for a good performance [25], [33] can be shortened by 60% to $0.06\lambda_0$, and this allowed for more space for the required directors.

This technique also allowed for an improvement in the front-to-back ratio, increasing the directivity with just three directors [24]. Basically, the surface reactance is modified as desired by the addition of a finite periodic grid of metallic strips in the y-direction (see Fig. 2 (a)). The length of these metallic strips L_{AD} was kept constant for all directors. This is because the width W_{ADn} is the main factor influencing the capacitive coupling and thus increasing the effective relative permittivity near the driven and parasitic elements. It should also be mentioned, that during our many optimisations and simulation studies using CST microwave studio [34], it was found that the best antenna performance (in terms of matching and directivity) was achieved when W_{AD1}, W_{AD2}, and W_{AD3} were positioned near the directors.

The final parameters for the miniaturized antenna can be found in Table 1, where they are also compared to the original, non-miniaturized structure. It can also be observed that the parameter L_{yagi} was miniaturized, requiring a length of $0.35\lambda_0$ which is about a 60% reduction when compared to the conventional version ($0.58\lambda_0$). Also, due to the improvement of the front-to-back ratio and the meandering of the driven element, the reflector implemented on the ground plane can be further reduced to a third in width W_{ref} and a half in length L_{ref} when compared to the non-miniaturized version (see Table 1). This supported further compactness.
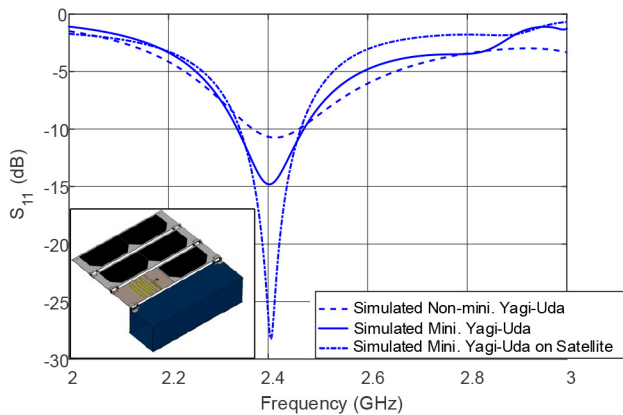
FIGURE 4. Simulated reflection coefficient for the different Yagi-Uda antennas: the conventional non-miniaturized Yagi-Uda (blue dashed line); the miniaturized antenna in free-space (solid blue line), and the miniaturized Yagi-Uda integrated on the PicoSat Unicorn-2 chassis (blue dotted line). The bottom left inset depicts the simulated model of the proposed antenna on the SmallSat chassis.
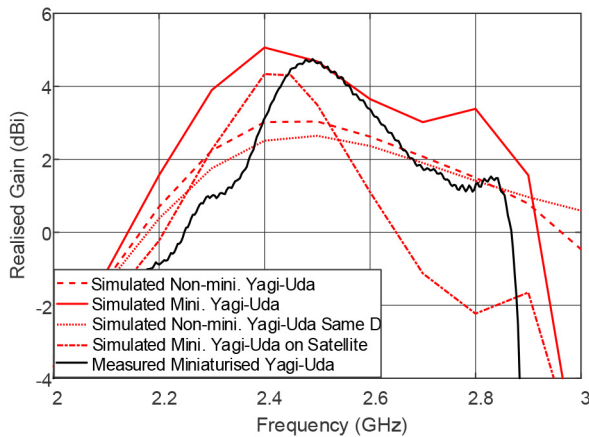
FIGURE 5. Simulated realized gain at full end-fire ($\theta = 90°$, $\phi = 90°$) versus frequency for the different Yagi-Uda antennas: the conventional non-miniaturized (red dashed line); the miniaturized antenna using artificial dielectrics concepts (red solid line), simulation results of a conventional Yagi-Uda with the distance between directors D reduced to the values employed by the miniaturized case (dotted red line) and the miniaturized antenna integrated on the satellite chassis (dotted-dashed red line). Additionally, measured results for the miniaturized Yagi-Uda antenna (solid black line) are also included.

The two designs are also placed side-by-side in Fig. 3 for size comparison.

B. SIMULATION RESULTS

A comparison of the reflection coefficients for the non-miniaturized and the miniaturized antennas is reported in Fig. 4. The miniaturized design offers a better impedance matching ($|S_{11}| \leq -15$ dB) although the -10 dB bandwidth over the required S-band operating frequency range is very similar for both cases and compliant with specifications required for the Unicorn-2 PicoSat.

In Fig. 5, the simulated realized gain values at full end-fire ($\theta = 90°$, $\phi = 90°$) are reported for the two configurations. The standard Yagi-Uda antenna provides a peak gain of around 3 dBi while, thanks to the improvement of the front-to-back ratio due to the controlled surface reactance,

TABLE 2. Yagi-Uda original & miniaturized performance comparison.

	Impedance Bandwidth	Peak Realised Gain (dBi)	Peak Total Efficiency
Conventional	4%	3.07	86.9%
Miniaturized	5.8%	5.06	89.1%

	Front-to-Back Ratio (dB)	Max. Beam Direction	Half-Power Beamwidth
Conventional	1.8	86°	186.2°
Miniaturized	3.5	92°	119.1°

the miniaturized antenna has a simulated realized gain of 5.1 dBi, also complying with the requirements. Additionally, the distance D between the directors in the non-miniaturized case has been reduced to the dimensions of the miniaturized antenna (from $0.15\lambda_0$ to $0.06\lambda_0$) to show the difference in performance and the need to include the reactive loading of the 1-D artificial dielectric structures for efficient radiation in a constrained footprint. It is shown in Fig. 5 that the realized gain is even lower than in the standard case as it does not comply with the required theoretical values for D, which is usually 0.15 to $0.3\lambda_0$ due to the effective coupling between directors. The performance comparison between the miniaturized and non-miniaturized version is reported in Table 2.

Furthermore, the miniaturized antenna has been simulated on the lossy polyamide PicoSat chassis (see Fig. 1 and Fig. 4, inset), where a UFL connector is used for surface mount feeding. Initial analysis were carried out in [18], where the antenna was simulated next to a PEC satellite body. This deviated the beam towards $\theta = 100°$ and reduced the gain to 3 dBi at full end-fire. The material of the body has been updated according to Alba Orbital instructions and lossy polyamide carbon fiber has been used. As shown in Fig. 4, the antenna offers reflection coefficient values up to -25 dB with a slightly diminished bandwidth of 5.13%. In this case, the beam is still pointing towards full end-fire ($\theta = 90°$, $\phi = 90°$) with gain values of 4.3 dBi as depicted in Fig. 5. There is a reduction of around 0.7 dBi with respect to the non-integrated scenario. This degradation in gain is caused by the addition of the connector and the influence of the body of the satellite and the metallic surroundings. This loss could be compensated by the addition of another director in the space available.

III. EXPERIMENTAL RESULTS

The miniaturized Yagi-Uda S-band planar antenna was manufactured using an FR-4 substrate ($\epsilon_r = 4.4$) having a thickness of 0.4 mm, and dimensions of $43.80 \times 50\,\text{mm}^2$ for low-cost experimental testing and simple integration with the existing FR-4 solar panel array. It should be mentioned that FR-4 dielectric properties may not be stable in harsh environments such as space and could degrade antenna radiation characteristics. Basically, non-space qualified FR-4
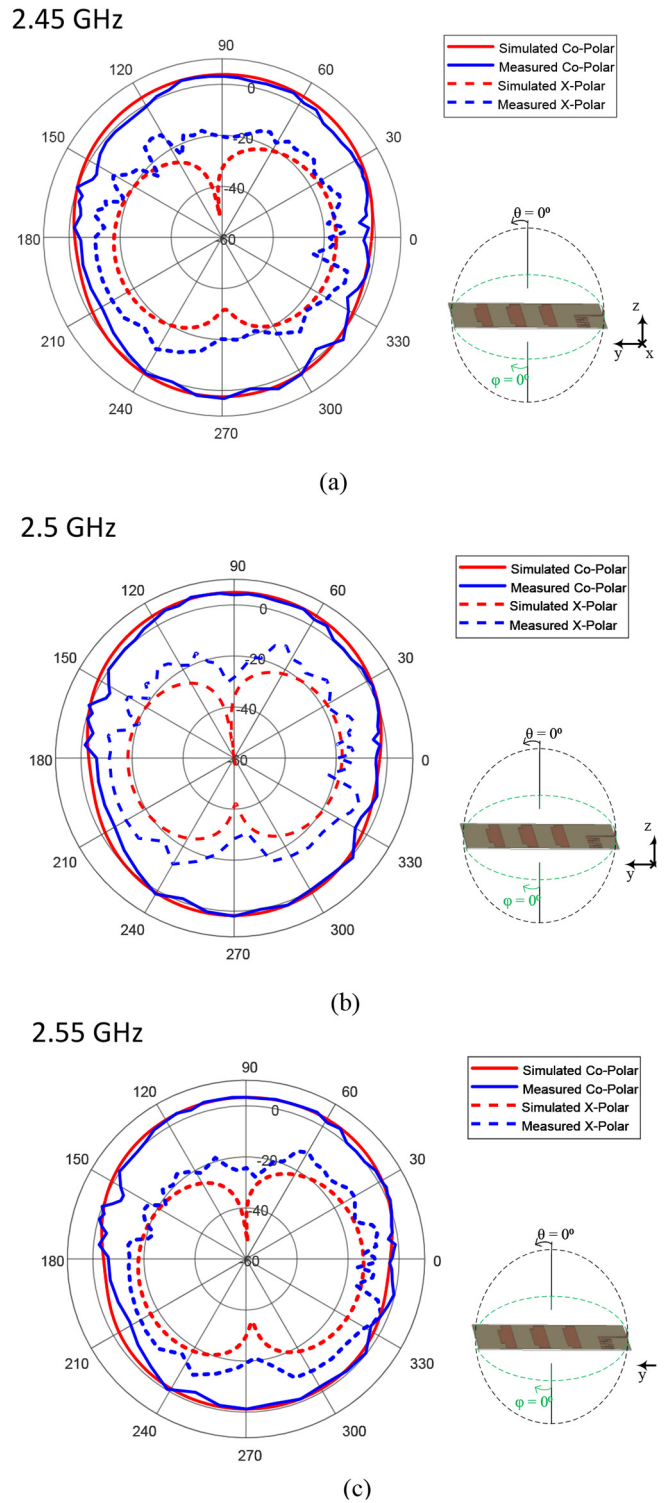
Top View   Bottom View

(a)

(b)
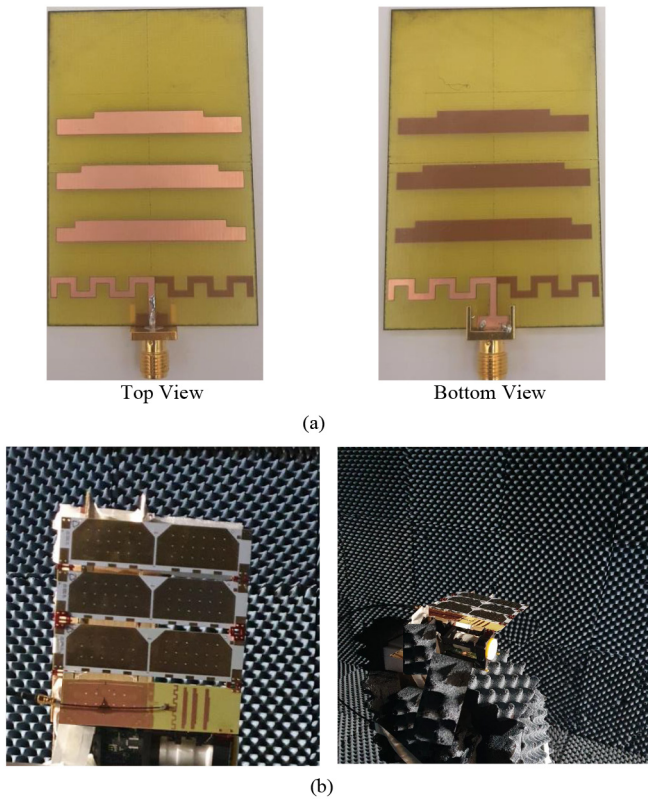
FIGURE 6. (a) Top and bottom views for the (manufactured) miniaturized Yagi-Uda antenna with artificial dielectric loading and meandering implemented using a 0.4 mm thick FR-4 substrate; (b) integrated Yagi-Uda antenna for placement on the PicoSat Unicorn-2 and testing.
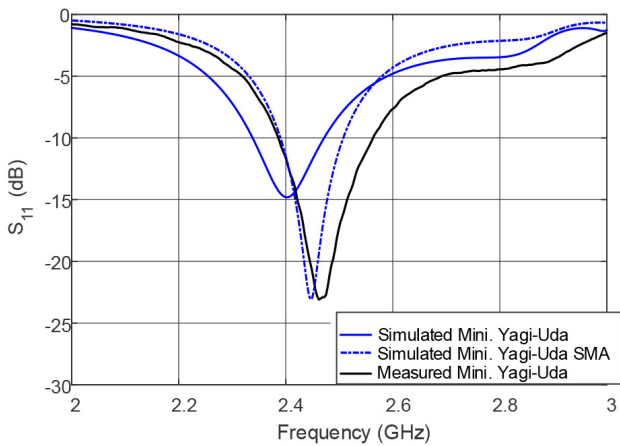
FIGURE 7. Reflection coefficient for the miniaturized Yagi-Uda antenna: the simulated miniaturized antenna reported in Fig. 4 (blue solid line), the miniaturized antenna design including an SMA connector (blue dash-dotted line) for accurate comparison with the measured prototype, see Fig. 6(a) (black solid line).

2.45 GHz

(a)

2.5 GHz

(b)

2.55 GHz

(c)

FIGURE 8. Miniaturized Yagi-Uda antenna radiation patterns in the $\phi = 90°$ plane at different frequencies. (a) Measured results plotted at 2.45 GHz; (b) measured results plotted at 2.5 GHz where the maximum measured gain is achieved due to the noted frequency shift; and (c) measured results plotted at 2.55 GHz.

PCB laminates may not maintain stable physical properties at extremely low or high temperatures. Further design work using space qualified TMM4 laminates from Rogers, which have low thermal variations and similar electric properties to FR-4, together with a metal coating additive (e.g., Alodine 1200 to help with corrosion resistance), could be used in future to maintain performance making the design more suitable and robust for space and other harsh operating environments.

**TABLE 3.** Simulated & measured performance comparison for the miniaturized Yagi-Uda planar antenna.

	Impedance Bandwidth	Peak Realized Gain (dBi)	Peak Radiation Efficiency
Simulated	5.8%	5.06	90.1%
Measured	6.25%	4.76	84.1%

This PCB antenna is depicted in Fig. 6 (a) and the measured reflection coefficient results are reported in Fig. 7. There is a shift in frequency towards 2.45 GHz due to the addition of an SMA connector. Simulations have been repeated including the connector and, as it is shown in Fig. 7, the minimum of the reflection coefficient for the antenna is shifted to 2.45 GHz. Regardless, simulations and measurements are in good agreement (when including the connector in the simulation model) with $|S_{11}| \leq 20$ dB with a measured -10 dB impedance bandwidth of 6.25%.

Far-field measurements have been carried out in an anechoic chamber. It should be noted that the far-field positioner had an impact on the radiation pattern measurements shifting the resonance frequency for the compact antenna (similar to [38]). This is specific to the measurement setup available, and could be avoided in other measurement facilities. Polar plots, comparing the simulated and measured results for the miniaturized antenna from 2.45 GHz to 2.55 GHz, are reported in Fig. 8 where the simulation model is shown for reference. The expected performance is observed for the realized gain (Figs. 5 and 8) with a loss of 0.3 dB (4.76 dBi) at the maximum peak realized gain frequency of 2.5 GHz (when compared to the simulated case). Also, the radiation pattern displays a broad-beam shape. However, the main lobe is maximum along the axis of the antenna ($\theta = 90°$) (see axis definition in Fig. 8) while gain values of -3 dBi are achieved at broadside, indicating end-fire performance. The front-to-back ratio is about 3.5 dB. Results for the cross-polarization levels are also shown and are below -25 dB at the end-fire and back-fire directions. A summary of the measured values with a comparison with simulation results has been reported in Table 3.

A new prototype has been also manufactured to be fully integrated on the deployable wing of the PicoSat Unicorn-2. This prototype is depicted in Fig. 6 (b). As it can be observed, a defected ground plane has been added at the back of the design to emulate the effects of a solar cell. The simulated and measured results for the co- and cross-polar radiation patterns of the antenna integrated on the chassis at 2.4 GHz for the $\phi = 90°$ plane are depicted in Figs. 9 and 10. Both polarizations agree well, showing maximum gain values of 4.9 dBi for the co-polar component and a improved front-to-back ratio of 10 dB. Cross-polar levels are higher with respect to the non-integrated version (Fig. 8) due to the additional metallic bodies surrounding the compact antenna.

A comparison has been included in Table 4, where the advantages of our proposed antenna are highlighted when compared to other state-of-the-art compact designs. Most of
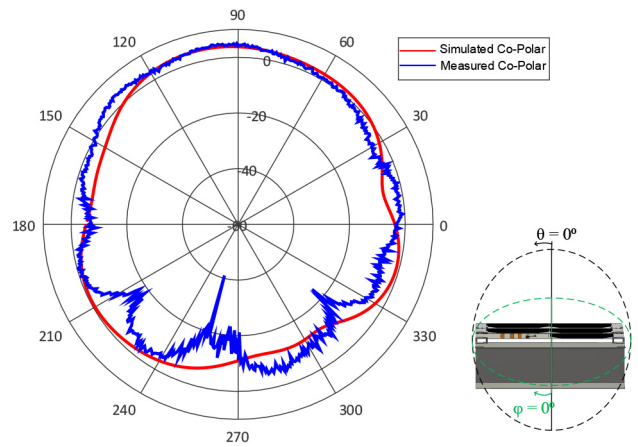
FIGURE 9. Co-polar radiation pattern for the simulated (red line) and measured (blue line) miniaturized Yagi-Uda antennas integrated on the satellite chassis at 2.4 GHz ($\phi = 90°$ plane).
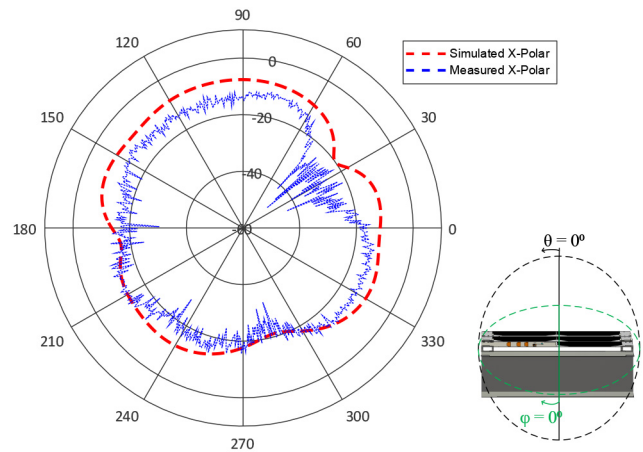
FIGURE 10. Cross-polar radiation pattern for the simulated (red line) and measured (blue line) miniaturized Yagi-Uda antennas integrated on the satellite chassis at 2.4 GHz ($\phi = 90°$ plane).

these works are based on WLAN and similar applications, however existing Yagi-Uda antennas for CubeSats [26], [27] have also been included in Table 4 to highlight the novelty in our integration approach for small satellites (in that the existing solar cell array of the Unicorn-2 PicoSat spacecraft is exploited) without requiring independent deployable systems for just the antenna. It should also be noted that the proposed three-director design achieves a competitive size when compared with systems of only one or no directors [29], [30], [31], [32], without sacrificing performance, bandwidth, or involving complex parasitic loading configurations such as parasitic interdigitated strips. Moreover, these previous works achieve the miniaturisation in one dimension only, while our proposed design is reduced in length and width by combining 1-D artificial dielectric loading and structure meandering.

IV. CONCLUSION
A planar miniaturized end-fire Yagi-Uda for PicoSat or other SmallSat integration was proposed which can support placement within deployable solar panel arrays.

TABLE 4. Comparison of state-of-the-art planar Yagi-Uda antennas.

Ref.	Miniaturization Technique	Freq. (GHz)	Relative Permittivity	Size (λ_0)	Number of Directors	Bandwidth	Application	Integration
[26]	None	2.47	4.4	$0.81 \times 1.4 \times 0.03$	3	5.42% (Sim.)	CubeSat	Attached
[27]	None	2.45	4.4	$0.66 \times 0.66 \times 0.005$	1	8.16% (Meas.)	CubeSat	Deployable
[28]	Meandering and Artificial Transmission Lines	5.5	3.38	$0.56 \times 0.79 \times 0.009$	1	33% (Meas.)	WLAN	-
[29]	Meandering	0.92	-	0.25×0.14	0	-	RFID	-
[30]	Folded Dipole	2.4	4.3	$0.42 \times 0.51 \times 0.012$	1	7.7% (Meas.)	WLAN	-
[31]	C-shaped Dipoles	2.45	4.4	$0.4 \times 0.48 \times 0.012$	1	40.7% (Sim.)	WLAN	-
[32]	Parasitic Interdigitated Strip	1.48	2.2	$0.57 \times 0.12 \times 0.002$	0	7.1% (Meas.)	-	-
[37]	Stepped-width Reflector	2.4	3.8	$0.4 \times 0.48 \times 0.006$	1	10.4% (Meas.)	-	-
This Work	Meandering and 1-D Artificial Dielectric Concepts	2.4	4.4	$0.35 \times 0.35 \times 0.003$	3	6.25% (Meas.)	PicoSat	Fully Integrated

Miniaturization techniques based on artificial dielectric concepts and meandering dipoles have also been employed to reduce key antenna parameters, such as the distance required between directors or the length required for the driven element to operate at 2.4 GHz, from $0.15\lambda_0$ to $0.06\lambda_0$ and from $0.21\lambda_0$ to $0.17\lambda_0$ respectively, when compared to a more conventional planar Yagi-Uda antenna. Regardless of this reduction, RF performance of the antenna is still maintained and with an improvement in the front-to-back ratio that allows for higher gain. Also, the minimum length of substrate to accommodate the antenna is reduced from $0.58\lambda_0$ to $0.35\lambda_0$.

As reported in the paper, efficient antenna performance was achieved by complying with the restricted dimensions of the FR-4 substrate under the solar cells. Measured realized gain values are about 5 dBi which are in agreement with the simulations for the antenna fully integrated on the satellite chassis. Performance of the compact antenna could be further improved by the addition of a fourth director and artificial dielectric element for compactness. This low-cost planar antenna can also be useful for CubeSats and other SmallSats, and generally where compact and low-profile antenna elements are needed to generate end-fire radiation.

ACKNOWLEDGMENT

REFERENCES

[1] A. Toorian, K. Diaz, and S. Lee, "The CubeSat approach to space access," in *Proc. IEEE Aerosp. Conf.*, Mar. 2008, pp. 1–14.

[2] "CubeSat design specification, rev. 13." Apr. 2015. [Online]. Available: http://www.cubesatorg

[3] V. Gómez-Guillamón Buendía, S. Liberto, G. Goussetis, and N. J. G. Fonseca, "Review of antenna technologies for very high frequency data exchange systems," *Int. J. Satell. Commun. Netw.*, pp. 1–12, Sep. 2021.

[4] "Helios deployable antenna." CubeSatShop. Accessed: Oct. 5, 2022. [Online]. Available: https://www.cubesatshop.com/product/helios-deployable-antenna/

[5] S. K. Podilchak, A. P. Murdoch, and Y. M. M. Antar, "Compact, microstrip-based folded-shorted patches: PCB antennas for use on microsatellites," *IEEE Antennas Propag. Mag.*, vol. 59, no. 2, pp. 88–95, Apr. 2017.

[6] S. K. Podilchak et al., "A compact circularly Polarized antenna using an array of folded-shorted patches," *IEEE Trans. Antennas Propag.*, vol. 61, no. 9, pp. 4861–4867, Sep. 2013.

[7] "Alba Orbital, Unicorn-2 mission ideas." Accessed: Oct. 5, 2022. [Online]. Available: http://www.albaorbital.com/unicorn2-mission-ideas

[8] N. Chahat, R. E. Hodges, J. Sauder, M. Thomson, E. Peral, and Y. Rahmat-Samii, "CubeSat deployable Ka-band mesh reflector antenna development for earth science missions," *IEEE Trans. Antennas Propag.*, vol. 64, no. 6, pp. 2083–2093, Jun. 2016.

[9] A. Babuscia, B. Corbin, M. Knapp, R. Jensen-Clem, M. Van de Loo, and S. Seager, "Inflatable antenna for Cubesats: Motivation for development and antenna design," *Acta Astronautica*, vol. 91, pp. 322–332, Nov. 2013.

[10] S. Vaccaro, J. R. Mosig, and P. de Maagt, "Two advanced solar antenna "SOLANT" designs for satellite and terrestrial communications," *IEEE Trans. Antennas Propag.*, vol. 51, no. 8, pp. 2028–2034, Aug. 2003.

[11] O. Yurduseven and D. Smith, "A solar cell stacked multi-slot quad-band PIFA for GSM, WLAN and WiMAX networks," *IEEE Microw. Wireless Compon. Lett.*, vol. 23, no. 6, pp. 285–287, Jun. 2013.

[12] E. Escobar, N. Kirsch, G. Kontopidis, and B. Turner, "5.5 GHz optically transparent mesh wire microstrip patch antenna," *Electron. Lett.*, vol. 51, no. 16, pp. 1220–1222, 2015.

[13] T. W. Turpin and R. Baktur, "Meshed patch antennas integrated on solar cells," *IEEE Antennas Wireless Propag. Lett.*, vol. 8, pp. 693–696, 2009.

[14] S. K. Podilchak et al., "Solar-panel integrated circularly polarized meshed patch for Cubesats and other small satellites," *IEEE Access*, vol. 7, pp. 96560–96566, 2019.

[15] N. Neveu, M. Garcia, J. Casana, R. Dettloff, D. R. Jackson, and J. Chen, "Transparent microstrip antennas for CubeSat applications," in *Proc. IEEE Int. Conf. Wireless Space Extreme Environ.*, Nov. 2013, pp. 1–4.

[16] S. Y. Lee, M. Choo, S. Jung, and W. Hong, "Optically transparent nano-patterned antennas: A review and future directions," *Appl. Sci.*, vol. 8, no. 6, p. 901, Aug. 2018.

[17] S. Tariq and R. Baktur, "Circularly polarized UHF up-and downlink antennas integrated with CubeSat solar panels," in *Proc. IEEE Int. Symp. Antennas Propagat. USNC/URSI Nat. Radio Sci. Meeting*, 2015, pp. 1424–1425.

[18] V. Gómez-Guillamón Buendía et al., "Compact end-fire antenna designs for PicoSat integration and other small satellite missions," in *Proc. 50th Eur. Microw. Conf. (EuMC)*, 2021, pp. 463–466.

[19] H. Yang, M. You, W. Lu, L. Zhu, and H. Zhu, "Envisioning an endfire circularly polarized antenna: Presenting a planar antenna with a wide beamwidth and enhanced front-to-back ratio," *IEEE Antennas Propag. Mag.*, vol. 60, no. 4, pp. 70–79, Aug. 2018.

[20] M. You, W. Lu, B. Xue, L. Zhu, and H. Zhu, "A novel planar endfire circularly polarized antenna with wide axial-ratio beamwidth and wide impedance bandwidth," *IEEE Trans. Antennas Propag.*, vol. 64, no. 10, pp. 4554–4559, Oct. 2016.

[21] B. Xue, M. You, W.-J. Lu, and L. Zhu, "Planar endfire circularly polarized antenna using concentric annular sector complementary dipoles," *Int. J. RF Microw. Comput.-Aided Eng.*, vol. 26, no. 9, pp. 829–838, 2016.

[22] L. J. Foged et al., "Miniaturized array antenna using artificial magnetic materials for satellite-based AIS system," *IEEE Trans. Antennas Propag.*, vol. 63, no. 4, pp. 1276–1287, Apr. 2015.

[23] S. Khan et al., "Miniaturization of dielectric resonator antenna by using artificial magnetic conductor surface," *IEEE Access*, vol. 8, pp. 68548–68558, 2020.

[24] W. H. Syed and A. Neto, "Front-to-back ratio enhancement of planar printed antennas by means of artificial dielectric layers," *IEEE Trans. Antennas Propag.*, vol. 61, no. 11, pp. 5408–5416, Nov. 2013.

[25] J. Floc'h, J. Denoual, and K. Sallem, "Design of printed dipole with reflector and multi directors," in *Proc. Loughborough Antennas Propagat. Conf.*, Nov. 2009, pp. 421–424.

[26] S. Liu, R. Raad, and F. E. M. Tubbal, "Printed Yagi-Uda antenna array on CubeSat," in *Proc. 11th Int. Conf. Signal Process. Commun. Syst. (ICSPCS)*, 2017, pp. 1–5.

[27] S. Liu, P. I. Theoharis, F. E. Tubbal, and R. Raad, "S-band steerable Yagi antenna for CubeSats," in *Proc. 13th Int. Conf. Signal Process. Commun. Syst. (ICSPCS)*, 2019, pp. 1–5.

[28] T.-G. Ma, C.-W. Wang, R.-C. Hua, and J.-W. Tsai, "A modified quasi-Yagi antenna with a new compact microstrip-to-coplanar strip transition using artificial transmission lines," *IEEE Trans. Antennas Propag.*, vol. 57, no. 8, pp. 2469–2474, Aug. 2009.

[29] J.-H. Kim, M.-G. Jeong, S.-H. Bae, and W.-S. Lee, "Miniaturized printed YAGI-Uda antenna with high directivity for long range UHF RFID item tracking systems," *Microw. Opt. Technol. Lett.*, vol. 59, no. 2, pp. 439–441, 2017.

[30] M. Farran et al., "Compact quasi-Yagi antenna with folded dipole fed by tapered integrated balun," *Electron. Lett.*, vol. 52, no. 10, pp. 789–790, 2016.

[31] J. Wu, Z. Zhao, Z. Nie, and Q. H. Liu, "A broadband unidirectional antenna based on closely spaced loading method," *IEEE Trans. Antennas Propag.*, vol. 61, no. 1, pp. 109–116, Jan. 2013.

[32] Y. Juan, W. Che, Z. N. Chen, and W. Yang, "A longitudinally compact Yagi–Uda antenna with a parasitic interdigital strip," *IEEE Antennas Wireless Propag. Lett.*, vol. 16, pp. 2618–2621, 2017.

[33] C. A. Balanis, *Antenna Theory: Analysis and Design*. New York, NY, USA: Wiley, 2016.

[34] "CST microwave studio." Accessed: Oct. 5, 2022. [Online]. Available: https://www.cst.com

[35] J. C. Peuzin and J. C. Gay, "Demonstration of the waveguiding properties of an artificial surface reactance," *IEEE Trans. Microw. Theory Techn.*, vol. 42, no. 9, pp. 1695–1699, Sep. 1994.

[36] R. King, D. Thiel, and K. Park, "The synthesis of surface reactance using an artificial dielectric," *IEEE Trans. Antennas Propag.*, vol. 31, no. 3, pp. 471–476, May 1983.

[37] Y. Luo and Q.-X. Chu, "A Yagi–Uda antenna with a stepped-width reflector shorter than the driven element," *IEEE Antennas Wireless Propag. Lett.*, vol. 15, pp. 564–567, 2016.

[38] Y. Li, S. K. Podilchak, D. E. Anagnostou, C. Constantinides, and T. Walkinshaw, "Compact antenna for Picosatellites using a meandered folded-shorted patch array," *IEEE Antennas Wireless Propag. Lett.*, vol. 19, no. 3, pp. 477–481, Mar. 2020.

SYMON K. PODILCHAK (Senior Member, IEEE) received the B.A.Sc. degree in engineering science from the University of Toronto, Toronto, ON, Canada, in 2005, and the M.A.Sc. and Ph.D. degrees in electrical engineering from Queen's University, Kingston, ON, Canada, in 2008 and 2013, respectively.

From 2013 to 2015, he was an Assistant Professor with Queen's University. In 2015, he joined Heriot–Watt University, Edinburgh, U.K., as an Assistant Professor, and became an Associate Professor, in 2017. He was a Lecturer with the European School of Antennas. He is currently a Senior Lecturer with the School of Engineering, The University of Edinburgh, Edinburgh. His research interests include surface waves, leaky-wave antennas, metasurfaces, UWB antennas, phased arrays, and RF integrated circuits. He has had industrial experience as a Computer Programmer, and has designed 24- and 77-GHz automotive radar systems with Samsung and Magna Electronics. His recent industry experiences also include the design of high-frequency surface-wave radar systems, professional software design, and implementation for measurements in anechoic chambers for the Canadian Department of National Defense and the SLOWPOKE Nuclear Reactor Facility. He has also designed compact antennas for wideband military communications, highly compact circularly polarized antennas for CubeSats with COM DEV International (currently, Honeywell) and The European Space Agency, and new wireless power transmission systems for Samsung.

Dr. Podilchak is leading a team of about ten Ph.D. students and academic researchers. He and his students have been the recipient of many best paper awards and scholarships, most notably Research Fellowships from the IEEE Antennas and Propagation Society, the IEEE Microwave Theory and Techniques Society, the European Microwave Association, and six Young Scientist Awards from the International Union of Radio Science. He was the recipient of the Postgraduate Fellowship from the Natural Sciences and Engineering Research Council of Canada. In 2011, 2013, 2020, and 2021, he and his students received Student Paper Awards at the IEEE International Symposium on Antennas and Propagation; in 2012, the Best Paper Prize for Antenna Design at the European Conference on Antennas and Propagation for his work on CubeSat antennas, and in 2016, the European Microwave Prize for his research on surface waves and leaky-wave antennas. In 2017 and 2019, he was bestowed a Visiting Professorship Award at Sapienza University, Rome, Italy, and from 2016 to 2019, his research was supported by a H2020 Marie Sklodowska-Curie European Research Fellowship. He was recognized as an outstanding reviewer of the IEEE TRANSACTIONS ON ANTENNAS AND PROPAGATION, in 2014 and 2020. In 2021, he was the recipient of the COVID-19 Above and Beyond Medal for leading research on remote microwave sterilization of the coronavirus. He was also the Founder and the First Chairman of the IEEE AP-S and IEEE MTT-S Joint Chapters in Canada and Scotland, in 2014 and 2019, respectively. In recognition of these services, he was presented with an Outstanding Volunteer Award from IEEE in 2015, and in 2020 and 2021, MTT-S and AP-S, respectively, recognized this Scotland Chapter for its activities and it was awarded the winner of the Outstanding Chapter Award hosted by these two IEEE Societies. He was also the recipient of the Outstanding Dissertation Award for his Ph.D. degree. He was an Associate Editor for the *IET Electronics Letters*. He was a Guest Associate Editor of the IEEE OPEN JOURNAL OF ANTENNAS AND PROPAGATION and IEEE ANTENNAS AND WIRELESS PROPAGATION, and is currently serving as an Associate Editor for the IEEE TRANSACTIONS ON ANTENNAS AND PROPAGATION. He is also a Registered Professional Engineer.

VICTORIA GÓMEZ-GUILLAMÓN BUENDÍA (Member, IEEE) received the telecommunications engineering degree from the Technical University of Cartagena, Cartagena, Spain, in 2015, and the Ph.D. degree from Heriot–Watt University (HWU), Edinburgh, U.K., in 2019. She received different awards from HWU in appreciation of her research performance and innovative ideas. She became a Research Associate with HWU, where she participated in different projects funded by the European Space Agency focusing on the design of small antennas for CubeSat platforms. In 2021, she joined the Radar Technology Department, TNO, The Hague, The Netherlands, as an Antenna Scientist Innovator. She currently works on phased arrays for antenna-in-package technology for 5G/6G applications, EM interaction with human body and RCS reduction techniques. Her research interests also include leaky-wave antennas, surface-wave control, transparent antennas, and millimeter-wave systems.

SALVATORE LIBERTO (Student Member, IEEE) received the B.Eng. and M.Sc. degrees in electronic and telecommunications engineering from the University of Calabria in 2016 and 2019, respectively. In 2018, he was enrolled as a Visiting Scholar with Heriot–Watt University working on phased array antennas at Ka-band. He is currently pursuing the Ph.D. degree on the development and manufacture of an MEMS-based phased array antenna. His research interest covers phased array antennas, antenna systems for CubeSat application, RF passive components, and high-frequency PCB technology.

TOM WALKINSHAW is the Founder of Alba Orbital, a company focused on building prototype PocketQubes, started in 2012. He has more cumulative years developing PocketQubes than anyone else in the world and has led Alba to its position as the leading company in its field. He has won many awards and accolades, including the The Glasgow Caledonian University Alumni of the Year in 2019, 39th Coolest person in U.K. and Forbes 30 under 30, to name a few.

CONSTANTIN CONSTANTINIDES received the M.Sc. degree in signal and image processing in 2008, and the Ph.D. degree in image processing in 2012. He is an RF and Signal and Image Processing Engineer. After having studied in France, he went to Heriot–Watt University, Edinburgh, U.K., to work as a Researcher on leaky-wave and compact antennas starting in 2015. He worked in space-related projects, and then moved to Alba Orbital, Glasgow, a company that designs picosatellites, to work as an Engineer in 2017. He currently works on designing and optimizing antennas for picosatellites as well as working on satellite night imaging techniques.

DIMITRIS E. ANAGNOSTOU (Senior Member, IEEE) received the B.S.E.E. degree from the Democritus University of Thrace, Greece, in 2000, and the M.S.E.E. and Ph.D. degrees from the University of New Mexico, Albuquerque, NM, USA, in 2002 and 2005, respectively.

From 2005 to 2006, he was a Postdoctoral Fellow with the Georgia Institute of Technology, Atlanta, GA, USA. In 2007, he joined as an Assistant Professor with the South Dakota School of Mines and Technology, Rapid City, SD, USA, where he was promoted to an Associate Professor with tenure. In 2016, he joined the Institute of Signals, Sensors, and Systems, Heriot–Watt University, Edinburgh, U.K., where he is currently an Associate Professor. He has also worked with Kirtland AFB, Albuquerque, NM, USA, in 2011 as a AFRL Summer Faculty Fellow, and with the Democritus University of Thrace as an Assistant Professor. He has authored or coauthored more than 150 peer-reviewed journal and conference publications, and holds two U.S. patents on MEMS antennas and on optically scannable antennas. His research interests include reconfigurable antennas and arrays, miniaturized and electrically small antennas, antennas for wearable, space/satellite applications, radars and wireless sensing for assisted living, microwave circuits and packaging, and functional phase-change materials such as VO_2 for reconfigurable electronics, direct-write electronics on organics, RF-MEMS, and applications of artificial neural networks, deep learning, and signal processing in electromagnetics and healthcare. He has received the 2010 IEEE John D. Kraus Antenna Award, the 2011 DARPA Young Faculty Award by the U.S. Department of Defense, the 2014 Campus Star Award by the American Society for Engineering Education, the 2017 Young Alumni Award by the University of New Mexico, and four Honored Faculty Awards by SDSMT. Most recently, he received the prestigious H2020 Marie Skłodowska-Curie Individual Reintegration Fellowship for research on wireless vital sign monitoring. His students have also been recognized with IEEE and university awards (Engineering Prize, HWU, Best Ph.D. Thesis, SDSMT, and others). He serves or has served as an Associate Editor for the IEEE TRANSACTIONS ON ANTENNAS AND PROPAGATION from 2010 to 2016 and the *IET Microwaves, Antennas, and Propagation* since 2015. He was a Guest Editor of *IEEE Antennas and Wireless Propagation Letters* (Special Cluster on Antennas Using Advanced Materials). He is a member of the IEEE AP-S Educational Committee and the Technical Program Committee of the IEEE AP-S International Symposia. He is a member of the HKN Honor Society, ASEE, and the Technical Chamber of Greece (registered Professional Engineer).

GEORGE GOUSSETIS (Senior Member, IEEE) received the Diploma degree in electrical and computer engineering from the National Technical University of Athens, Greece, in 1998, the B.Sc. degree (First Class) in physics from University College London, U.K., in 2002, and the Ph.D. degree from the University of Westminster, London, U.K., in 2002. In 1998, he joined the Space Engineering, Rome, Italy, as a RF Engineer and in 1999 the Wireless Communications Research Group, University of Westminster as a Research Assistant. From 2002 to 2006, he was a Senior Research Fellow with Loughborough University, U.K. From 2006 to 2009, he was an Assistant Professor with Heriot–Watt University, Edinburgh, U.K., and an Associate Professor with Queen's University Belfast, U.K., from 2009 to 2013. In 2013, he joined Heriot–Watt University and was promoted to Professor in 2014. He currently directs the Institute of Sensors Signals and Systems with Heriot–Watt University. He has authored or coauthored over 500 peer-reviewed papers five book chapters one book and five patents. His research interests are in the area of microwave and antenna components and subsystems. He held research fellowships from the Onassis Foundation in 2001, the U.K. Royal Academy of Engineering from 2006 to 2011, and the European Commission Marie-Curie in 2011 and 2012 and again in 2014 and 2017. He is the co-recipient of the 2011 European Space Agency Young Engineer of the year prize, the 2011 EuCAP Best Student Paper Prize, the 2012 EuCAP Best Antenna Theory Paper Prize, and the 2016 Bell Labs Prize. He served as an Associate Editor for the IEEE ANTENNAS AND WIRELESS PROPAGATION LETTERS from 2014 to 2018.

MAARTEN VAN DER VORST received the M.Sc. and Ph.D. degrees in electrical engineering from the Eindhoven University of Technology, Eindhoven, The Netherlands, in 1995 and 1999, respectively. From 1999 to 2000, he worked with the TNO Physics and Electronics Laboratory, The Hague, The Netherlands, where the main topic was on Radar Cross-section calculations. In September 2000, he joined the Antenna Section of the European Space Agency. His current research interests include millimeter-wave and submillimeter-wave integrated antennas, radiometer and radar technology and the last eight years got involved in the additive manufacturing technology applied to antennas.